The evolution and termination of an iron-induced mesoscale bloom in the northeast subarctic Pacific

Philip W. Boyd and Robert Strzepek

NIWA Centre for Chemical and Physical Oceanography, Department of Chemistry, University of Otago, P.O. Box 56, Dunedin, New Zealand

Shigenobu Takeda

Department of Aquatic Bioscience, University of Tokyo, Bunkyo, Tokyo 113-8657, Japan

George Jackson

Department of Oceanography, Texas A&M University, College Station, Texas 77843-3146

C. S. Wong

Fisheries and Oceans Canada, Institute of Ocean Sciences, P.O. Box 6000, Sidney, British Columbia, V8L 4B2 Canada

R. Mike McKay

Department of Biological Sciences, Bowling Green State University, Bowling Green, Ohio 43403

Cliff Law

National Institute of Water and Atmospheric Research, 301 Evans Bay Parade, Greta Point, P.O. Box 14-901, Kilbirnie, Wellington, New Zealand

Hiroshi Kiyosawa

Marine Biological Research Institute of Japan, Shinagawa, Tokyo 142-0042, Japan

Hiroaki Saito

Tohoku National Fisheries Research Institute, Shiogama, Miyagi 985-0001, Japan

Nelson Sherry

Earth & Ocean Sciences, University of British Columbia, 6270 University Blvd, Vancouver, British Columbia, V6T 1Z4, Canada

Keith Johnson and Jim Gower

Fisheries and Oceans Canada, Institute of Ocean Sciences, P.O. Box 6000, Sidney, British Columbia, V8L 4B2 Canada

Neelam Ramaiah

Department of Aquatic Bioscience, University of Tokyo, Bunkyo, Tokyo 113-8657, Japan

Abstract

We initiated and mapped a diatom bloom in the northeast subarctic Pacific by concurrently adding dissolved iron and the tracer sulfur hexafluoride to a mesoscale patch of high-nitrate, low-chlorophyll waters. The bloom was dominated by pennate diatoms and was monitored for 25 d, which was sufficiently long to observe the evolution and termination of the bloom and most of the decline phase. Fast repetition–rate fluorometry indicated that the diatoms were iron-replete until day 12, followed by a 4–5-d transition to iron limitation. This transition period was characterized by relatively high rates of algal growth and nutrient uptake, which pointed to diatoms using intracellularly stored iron. By days 16–17, the bloom was probably limited simultaneously by both iron and silicic acid

supply, because low silicic acid concentrations were evident. Modeling simulations, using data from our study, provided an estimate of the critical threshold for algal aggregation. Observed diatom abundances during the bloom exceeded this threshold between days 13 and 17. Mass sedimentation of diatoms and diatom aggregates was recorded in surface-tethered free-drifting sediment traps at 50 m in depth on day 21. Although the termination of the bloom was probably controlled by the availability of both iron and silicic acid, we cannot rule out the role of algal aggregation. The bloom decline was likely triggered by the onset of mass sedimentation. During our study, evidence of both diatom species succession and species-specific aggregation point to important links between algal nutrient stress and the initiation of algal aggregation.

Phytoplankton blooms in both the coastal and open ocean play a major role in the biogeochemical cycling of elements such as carbon, nitrogen (Lochte et al. 1993), and silicon (Nelson et al. 2002). The evolution of algal blooms has been monitored using a range of approaches including field sampling (Riebesell 1991) and algal cultures in lab mesocosms (Alldredge et al. 1995; Prieto et al. 2002). However, each of these approaches—while yielding insights into aspects of bloom dynamics such as aggregation (Riebesell 1991; Alldredge et al. 1995)—suffer from experimental artefacts. Artefacts include hydrodynamic biases during lab mesocosm studies (Prieto et al. 2002) and the confounding influence of temporal and spatial variability on shipboard studies of blooms (Lochte et al. 1993). Many of these problems associated with the study of bloom dynamics have been overcome by using an approach advocated by Martin (1990)—the induction of blooms (by enriching high-nitrate, low-chlorophyll [HNLC] waters with dissolved iron) within a mesoscale patch of the surface ocean to which an inert tracer (sulfur hexafluoride, SF_6) is added concurrently and subsequently monitored.

The addition of iron to a suitable site in HNLC waters during mesoscale perturbation experiments provides both (1) the unambiguous means to study the bloom evolution from its onset and (2) insights into which environmental trigger initiates the bloom. This approach allows us to study holistically the development of blooms, with measurements ranging from algal physiology (Maldonado et al. 2002) to herbivory (Landry et al. 2000) to the downward export of particulates (Bidigare et al. 1999; Boyd et al. 2004). To date, nine mesoscale iron enrichments have been conducted in polar, subpolar, and tropical HNLC regions (Boyd 2004), with water temperatures ranging from <0°C to 25°C (Boyd 2004). These studies therefore provide insights into the timescales of bloom development across a wide range of environmental conditions. The majority of these nine experiments have resulted in conditions that permitted the study of only the evolution phase of the bloom (i.e., the period of increasing algal stocks). However, two experiments—IronEx II and Subarctic Ecosystem Response to Iron Enrichment Study (SERIES)—were able to investigate both the development and the latter phases of these blooms, such as termination (i.e., the inflection point between bloom evolution and decline) and decline (i.e., the period of decreasing algal stocks) (Boyd 2004). Thus, mesoscale iron enrichment experiments provide a platform to investigate the factor(s) that control each phase of a bloom and how they influence the biogeochemical signature of the bloom.

The factor(s) controlling the termination of an algal bloom may be bottom-up factors (such as nutrient supply) and/or top-down factors (such as herbivory) (Cullen 1991). These differing modes of control will also affect the rate of bloom decline and the fate of the bloom by setting the trophic pathways and hence the transfer of energy from the bloom (Banse 1991). Improved resolution of these latter bloom phases is needed to better understand the factors that set time lags between blooms and their subsequent fate—such as export to depth (Buesseler et al. 2001). Such data will assist biogeochemical modelers studying the role of iron in open ocean systems (Hannon et al. 2001). Mesoscale iron enrichments also offer clues as to how bloom dynamics might have been altered in the geological past, when there was evidence of an enhanced supply of resources such as iron (Martin 1990). Here, for the first time, we report in detail on the evolution and termination of an iron-induced diatom bloom in the HNLC waters of the northeast subarctic Pacific during the SERIES.

Materials and methods

Site selection—Prior to commencing the joint iron and SF_6 addition, we conducted a 48-h oceanographic survey (7 and 8 July 2002) in the vicinity of Ocean Station Papa (OSP, 50°N, 145°W; Fig. 1a) to identify an appropriate site with HNLC characteristics typical of this region (LaRoche et al. 1996; Nishioka et al. 2001). A suitable site (Table 1) was located 50 km northeast of OSP, and the surface waters were enriched on 10 July 2002 (denoted as day 0 of SERIES) with dissolved iron to >1 nmol L^{-1}, along with the concurrent addition of the tracer SF_6 (>400 fmol L^{-1}) following procedures reported in Law et al. (1998). Throughout SERIES, mixed-layer SF_6 concentrations were always significantly higher than background levels, and thus we did not add any more SF_6 to the patch. However, on day 6, a second iron infusion was required that raised dissolved iron by around 0.6 nmol L^{-1}.

Mapping the patch evolution—The physical evolution of the SF_6–labeled, iron-enriched patch was monitored daily during a 10–12-h shipboard underway survey (Boyd et al. 2004). During each overnight mapping survey, water was sampled from an intake 5 m subsurface for SF_6 (Law et al. 1998), temperature, and salinity (using a Seabird thermosalinograph); chlorophyll fluorescence (Boyd and Abraham 2001); macronutrients (Boyd et al. 2004); dissolved iron (Nishioka et al. 2001); and algal photosynthetic competence (F_v/F_m, using a fast repetition–rate fluorometer [FRRF], after Boyd and Abraham 2001). SERIES was a three-ship study, with two ships always being present at the study site, and so in some instances, measurements obtained during the un-
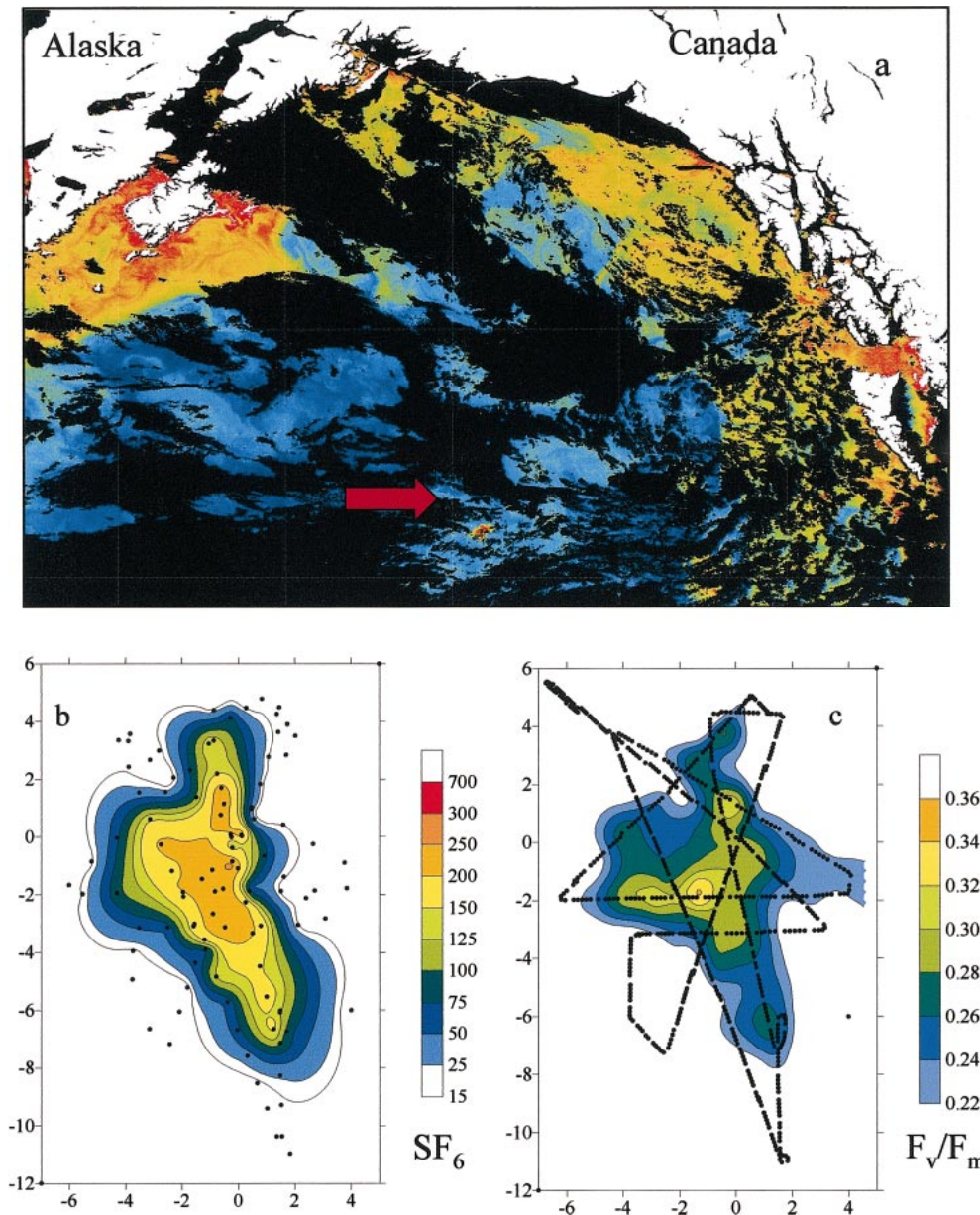
Fig. 1. (a) Map of northeast Pacific showing the SERIES site and the resulting phytoplankton bloom denoted by a red arrow, based on a SeaWiFS composite for July 2002; (b) survey map of SF_6 distributions on day 3 of SERIES; black dots are actual measurements; (c) corresponding lateral survey of F_v/F_m on day 3; black dots denote the sampling interval used in contour mapping.

derway surveys were made using different suites of instruments. Successful intercalibrations were conducted either prior to (e.g., dissolved iron) or during SERIES (e.g., FRRF). Our observations of this labeled patch concluded on 4 August 2002 (day 25).

Hydrographic sampling—Vertical profiles and water samples—for macronutrients, floristics, and particle characteristics—were taken daily from the upper 200 m of the water column using a Seabird CTD rosette at the center of the patch (defined each day by the highest SF_6 concentrations; Law et al. 1998) and were taken less frequently at an OUT

station in the surrounding HNLC waters at least 16 km from the patch periphery. Discrete samples were analyzed for SF_6 after the method of Law et al. (1998) and followed procedures for macronutrients (Boyd et al. 2004), biogenic silica (BSi; Boyd et al. 2004), and chlorophyll (Boyd and Abraham 2001). Concurrently sampled water was preserved in Lugols for light microscopic enumeration of diatoms (5-m depth only) and used for particle-size spectra analysis with a Sequoia LISST-25 after the method of Agrawal and Pottsmith (2000). Estimates of particulate organic carbon (POC) concentrations were obtained at 1 m in vertical resolution using a SeaTech beam transmissiometer in conjunction with the

Table 1. HNLC characteristics of upper ocean waters during an initial survey 50 km northeast of OSP that was selected ultimately as the SERIES site. Variations in macronutrient concentrations were due to the presence of a longitudinal gradient in the surrounding HNLC waters. F_v/F_m is the photosynthetic competence of the resident phytoplankton and is nondimensional. Flavodoxin levels in diatoms are a proxy for iron stress.

Parameter	Initial value
Mixed layer depth*	30 m
Temperature	12.5°C
Chlorophyll	0.35 μg L^{-1}
Nitrate	10–12 μmol L^{-1}
Silicic acid	14–16 μmol L^{-1}
Phosphate	>1 μmol L^{-1}
Dissolved iron	<0.1 nmol L^{-1}
F_v/F_m	0.24
Synechococcus	3×10^7 L^{-1}
Haptophytes	0.5×10^6 L^{-1}
Diatoms	4,800 L^{-1}
Dinoflagellates	1,800 L^{-1}
Flavodoxin levels	iron stressed†

* Denotes presence of a transient mixed layer to 10 m in depth from days 0 to 3 within the 25–30 m–deep seasonal mixed layer.
† Based on a comparison with previous shipboard studies that have shown that changes in flavodoxin levels have been successfully induced in this region (LaRoche et al. 1996).

POC-transmissivity algorithm of Bishop (1999): for justification of this approach, *see* Boyd et al. (2004). Vertically resolved samples for dissolved iron concentrations were taken using a trace metal clean Teflon pump and hosing (Nishioka et al. 2001). Intercalibration samples from a range of discrete depths in the mixed layer were exchanged between vessels, and intercalibrations showed good agreement (Boyd et al. 2004).

Algal physiological status—Several indices were used to monitor changes in algal physiological status following iron enrichment. Discrete samples from a range of depths in the mixed layer were analyzed for photosynthetic competence (F_v/F_m) of the phytoplankton community following procedures outlined in Boyd and Abraham (2001). Additional samples from 5 m in depth were analyzed for diatom flavodoxin, a proxy for the degree of iron stress in diatoms (LaRoche et al. 1996). For each sample, the flavodoxin levels were normalized to diatom abundance. These two indices provide different insights into the relationship between nutrient concentrations (in this case iron) and physiological status. Nutrient limitation—defined as a reduction in the growth rate of the phytoplankton community due to the low concentration of a nutrient (Sterner et al. 2004)—is assumed here to be reflected in F_v/F_m, whereas nutrient stress—defined as a physiological adjustment of an algal species to low nutrients, which may precede or occur with or without a reduction in growth rate (Sterner et al. 2004)—is assumed here to be best defined using flavodoxin. During SERIES we compared trends in both F_v/F_m and flavodoxin levels with those in algal growth rates to evaluate these assumptions.

Net phytoplankton growth rates were estimated daily using rates of primary production from 24-h simulated in situ incubations using ^{14}C, which are reported to approximate net primary production (NPP), in conjunction with algal biomass estimates based on carbon. Algal biomass was estimated using POC concentrations, as a carbon budget of the heterotrophic and autotrophic components of the food web during SERIES indicated that most of the increase in the mixed-layer POC inventory was attributable to phytoplankton stocks (Boyd et al. 2004). Previous data from OSP indicate that under ambient HNLC conditions, algal stocks comprise around 40% of POC concentrations (*see* Boyd et al. 2004). Thus, algal carbon for each day of SERIES was estimated as the daily mixed-layer POC concentration minus (0.6 $\times$ the initial POC concentration). Algal growth estimates were only computed until day 18 of SERIES, since after this time, there were large and sustained decreases in POC concentrations associated with the bloom decline. Algal carbon was also used to compute C:chlorophyll ratios, which were expressed as g:g.

As SERIES was conducted within an SF_6-labeled patch of water, it was possible to estimate phytoplankton nutrient uptake rates using nutrient concentration data. Uptake rates were estimated at the patch center by first subtracting the daily mean nutrient concentration from the initial nutrient concentration when the patch was first enriched with iron, then dividing by the number of days of SERIES that had elapsed. Nutrient uptake rates were subsequently corrected each day to take into account the enhancement of nutrient concentrations in the patch: increases in the patch size resulted from the entrainment of the surrounding HNLC waters, which are characterized (after day 2) by higher nutrient concentrations (Table 1). As the main aim of our study was to examine the mechanisms controlling the timing of different bloom phases, we have not corrected other data presented here, such as chlorophyll, POC, and BSi concentrations, for patch dilution.

Particle dynamics—The properties of phytoplankton cells, such as sinking rates, stickiness (α), and the production of transparent exopolymer particles (TEP), influence the downward export of particles during a bloom (Alldredge et al. 1995). Algal α is reported to influence aggregation directly, whereas TEP are thought to affect aggregation indirectly (Crocker and Passow 1995). To study the influence of particle dynamics on export, we collected particle samples and also conducted algal aggregation modeling studies. During SERIES, we obtained samples from 5 m in depth using the CTD rosette; the samples were analyzed for TEP abundance (Passow and Alldredge 1995) and for algal sinking rates (Bienfang 1981). As a result of logistical issues, in some cases—such as for algal sinking rates—samples were only collected on one vessel, and so data were available as a subset of the SERIES.

Algal aggregation is determined by the complex interplay of environmental conditions (including mixed-layer depth, shear) and algal properties such as growth rate, geometry, and α (Jackson and Lochmann 1992). During SERIES, the timing of aggregation by diatoms was explored using a coagulation model (Jackson and Lochmann 1992) in conjunction with inputted SERIES data on properties such as mixed-layer depth, initial abundance, and geometry of the dominant

diatoms; shear (predicted from meteorological data collected on SERIES); and algal growth rate (based on an exponential fit to trends in diatom abundances between days 3 and 12). Such a joint approach has predicted successfully, for two previous mesoscale iron enrichments, whether bloom conditions would result in aggregation as well as the timing of the onset of increased downward POC export (Boyd et al. 2002).

There have been no published studies on whether the α of open-ocean diatoms is altered by changes in either macronutrient and/or trace metal supply; hence, we had to assume a value of α in the model. We opted for a α value of one, based on a synthesis of lab-based and modeling studies (Jackson 2005), but also included a contrasting model simulation using a α value of 0.1, as has been reported for some coastal studies (*see* Jackson 2005). For SERIES, estimates of both the initiation of algal aggregation and subsequent increases in algal sinking rates were derived from a modified version of the model of Jackson and Lochmann (1992). This modification—the use of a 'composite' diatom geometry based on the mean equivalent spherical diameter of the main diatom species present during the bloom—was necessary, as the SERIES bloom was dominated by several pennate diatom species, whereas the original model was parameterized for an algal monoculture.

Results

Physical evolution of the labeled patch—The initial aerial extent of the iron-enriched HNLC waters was 77 km², but these iron-enriched waters extended only to 10 m in depth, as a transient mixed layer was present on day 0 within the 25–30-m deep seasonal mixed layer. Daily mapping surveys of surface waters indicated that the patch moved slowly northward and had increased in area to 88 km² by day 3 (Fig. 1b). The transient vertical structure in the mixed layer was eroded by day 3, and the seasonal mixed layer remained around 30 m for the duration of the experiment. The patch stretched into an ellipsoid along a north–south axis, increased in area to >200 km² by day 13, and grew to 1,000 km² by day 22, when the bloom was clearly visible from space (Fig. 1a). The entrainment of surrounding HNLC waters supplemented macronutrient supply, but reduced iron and chlorophyll concentrations at the patch center. Sharp lateral gradients in properties such as F_v/F_m, which corresponded to iron enrichment, were observed in transects through the patch (Fig. 1c).

Dissolved iron, chlorophyll, and macronutrient concentrations—Following iron enrichment, dissolved iron concentrations were initially raised by >1 nmol L^{-1} above ambient in a 10-m–thick surface layer within the seasonal mixed layer (Fig. 2a). On day 3, increased wind stress eroded this layer and thus decreased mixed-layer iron enrichment to <0.5 nmol iron (Fe) L^{-1}. Algal iron uptake and scavenging of iron onto particles probably contributed to a decrease in iron concentrations to <0.3 nmol L^{-1} by day 6, at which time a second iron infusion was carried out, resulting in iron enrichment of the mixed layer of 0.5 nmol Fe L^{-1} (Fig. 2a). Elevated iron concentrations resulted in a rapid increase in

chlorophyll to >2.0 μg L^{-1} by the time of the second iron infusion on day 6 (Fig. 2b). During this period of algal growth, there were corresponding reductions in nitrate, silicic acid, and phosphate of 3.5, 2.4, and 0.11 μmol L^{-1}, respectively (Fig. 2c,d). Primary production in the patch increased from initial rates of 0.3 g m^{-2} d^{-1} to >2 g carbon (C) m^{-2} d^{-1} by day 14 (data not shown). By day 12, dissolved iron concentrations in the patch were comparable to HNLC levels (i.e., <0.2 nmol L^{-1}; Nishioka et al. 2001), increases in chlorophyll were >2 μg L^{-1}, and nutrient depletion was around 5.0, 7.0, and 0.25 μmol L^{-1} for nitrate, silicic acid, and phosphate, respectively (Fig. 2c,d). Despite iron concentrations returning to background levels after day 12, chlorophyll concentrations continued to increase, peaking at >4.5 μg L^{-1} above background on days 16–17 and declining thereafter (Fig. 2a,b). By days 16–17, the blooming diatoms had depleted most of the mixed-layer silicic acid inventory (Fig. 2c), whereas around 3 μmol NO_3 L^{-1} remained. The bloom terminated on day 17, and chlorophyll concentrations rapidly declined by day 23 (Fig. 2b). Throughout the bloom evolution there were only minor changes in mixed-layer concentrations of dissolved iron, chlorophyll, and macronutrients in the HNLC waters surrounding the patch (Boyd et al. 2004).

Algal species composition and particle composition—The community at the iron enrichment site was dominated initially by *Synechococcus* and haptophytes such as autotrophic nanoflagellates (Table 1), with diatoms making a small contribution to algal stocks. Following iron enrichment, the observed increases in chlorophyll concentration between days 1 and 3 were mainly due to iron-elevated abundances of *Synechococcus* (Levasseur unpubl. data). There were subsequent increases, from days 4 to 11, in haptophyte abundances, which quadrupled to 2 × 10⁶ cells L^{-1} and were mainly due to increases in *Emiliana huxleyi* and, to a lesser extent, *Phaeocystis* spp. (Levasseur unpubl. data). *Synechococcus* abundances returned to ambient levels by day 4, as did haptophyte abundances by day 14 (Boyd et al. 2004). From days 1 to 5 there were few apparent changes in diatom stocks; however, after day 6, exponential increases in abundances were evident (Fig. 3a). Diatom stocks peaked on day 17 before subsequently declining. When we departed the site on day 25, diatom abundances were still greater than background abundances (Fig. 3a).

The bloom was not dominated by a single diatom species, with evidence of distinct peaks in *Chaetoceros* spp., *Thalassiosira* spp., and *Thalassiothrix longissima* over the 25 d of SERIES (Fig. 3a). Other diatom species that contributed to a lesser extent to the bloom include *Pseudo-Nitzschia* spp., *Neodenticula seminae,* and *Rhizosolenia* spp. During SERIES, increases in POC concentrations in the mixed layer generally followed the same temporal trends as for diatom abundances (Fig. 3), with the exception of the first 6–7 d, when nondiatom phytoplankton made a significant contribution to POC concentrations. As expected, temporal trends in mixed-layer BSi most closely corresponded to those for diatom abundances (Fig. 3b). BSi concentrations began to decline around day 17, as observed for POC concentrations and diatom abundances (Fig. 3). There was a greater than
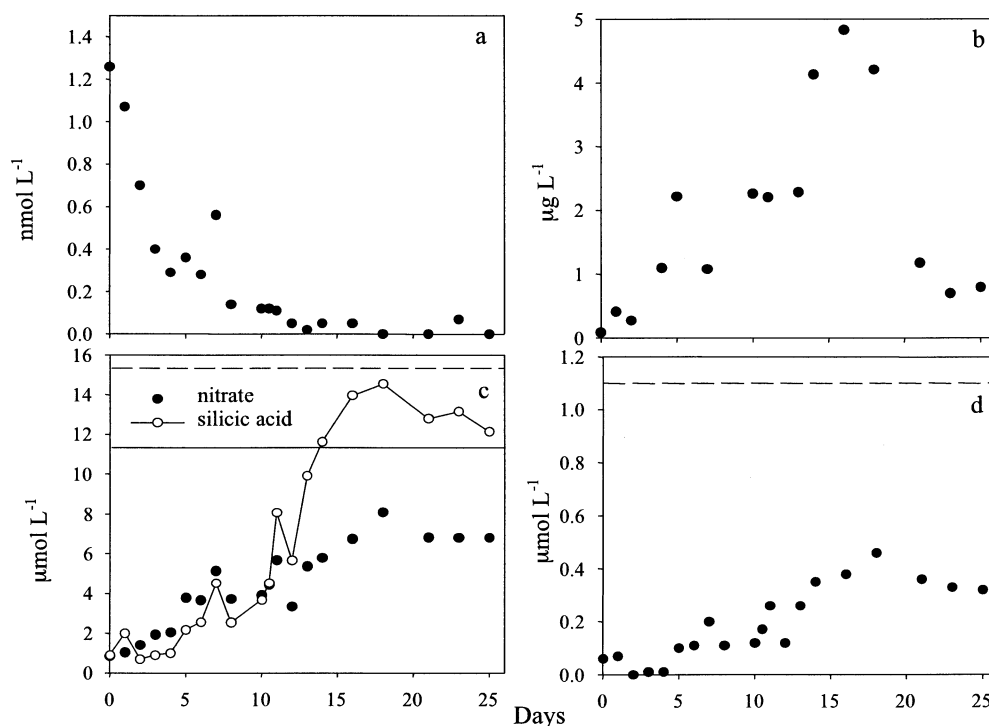
Fig. 2. (a) IN–OUT dissolved iron mixed-layer mean concentration; (b) IN–OUT chlorophyll mean mixed-layer concentrations; (c) OUT–IN nitrate and silicic acid mean mixed-layer concentrations. The initial nutrient concentrations are indicated by a long dashed line (silicic acid) and a medium dashed line (nitrate); (d) OUT–IN phosphate mean mixed-layer concentrations. The initial nutrient concentrations are indicated by a dashed line. The standard error of the mean ($n = 3$) for each property is smaller than the symbols. Dilution of the patch (which would reduce dissolved iron and chlorophyll concentrations and increase nutrient depletion was not corrected for, *see Methods*). The OUT data used for calculation of IN–OUT concentrations were based on the mean of four time points obtained between days 1 and 15 for dissolved iron, chlorophyll, and nutrient concentrations.

threefold range in the molar Si:C particulate ratios during the bloom (*see following*).

Algal physiological status—The F_v/F_m of the phytoplankton community in the patch displayed three distinct trends— a marked increase of iron enrichment within 24 h, then 11 d during which F_v/F_m varied little, followed by a persistent decline in F_v/F_m after day 12 (Fig. 4a). The relationship between F_v/F_m and dissolved iron concentrations was assessed using concurrent measurements derived from underway survey data on day 7. There was a marked threshold in F_v/F_m at around 0.2 nmol L^{-1} Fe, below which F_v/F_m was halved (Fig. 4b): on days 12–13, dissolved iron concentrations decreased to below this threshold and remained low (Fig. 2a), indicating that trends in F_v/F_m reflected iron rather than nutrient limitation. Diatom iron stress displayed four temporal trends during the evolution of the bloom (Fig. 4c). Within 24 h of iron enrichment, diatom iron stress was alleviated, but then it increased between days 3 and 5, even though iron concentrations were between 0.3 and 0.4 nmol L^{-1} (Fig. 2a). The second infusion of iron into the patch provided a transient alleviation of diatom iron stress, followed by the onset of marked iron stress, such that by day 11 flavodoxin levels

were comparable to those for resident diatoms in surrounding HNLC waters (Fig. 4c).

Iron supply elevated algal net growth rates, which had quadrupled by day 12 (Fig. 4d), and concurrently reduced the C:chlorophyll ratio from 120 to 40 (g:g) over this period (data not shown). The observed decrease in F_v/F_m from day 12 onward corresponded to a reversal in these iron-mediated changes in net growth rate (Fig. 4d) and in the C:chlorophyll ratio, which had increased to >100 by day 17. This transition from iron-replete to iron-limited conditions after day 12 (Fig. 4a) coincided with pronounced increases in the algal uptake ratio of Si:NO₃ from unity to three (Fig. 5). During SERIES, the increase in the Si:NO₃ uptake ratio was due primarily to elevated silicic acid uptake and, to a lesser extent, to a reduction in nitrate uptake (Fig. 5). This enhanced uptake of silicic acid resulted in the depletion of mixed-layer concentrations to <2 μmol L^{-1} by day 17 in spite of the resupply of silicic acid (mean supply was 0.5 μmol Si L^{-1} d^{-1}) to the patch as a result of lateral entrainment of HNLC waters.

Particle dynamics—During SERIES, there were pronounced temporal changes in particle properties. In several
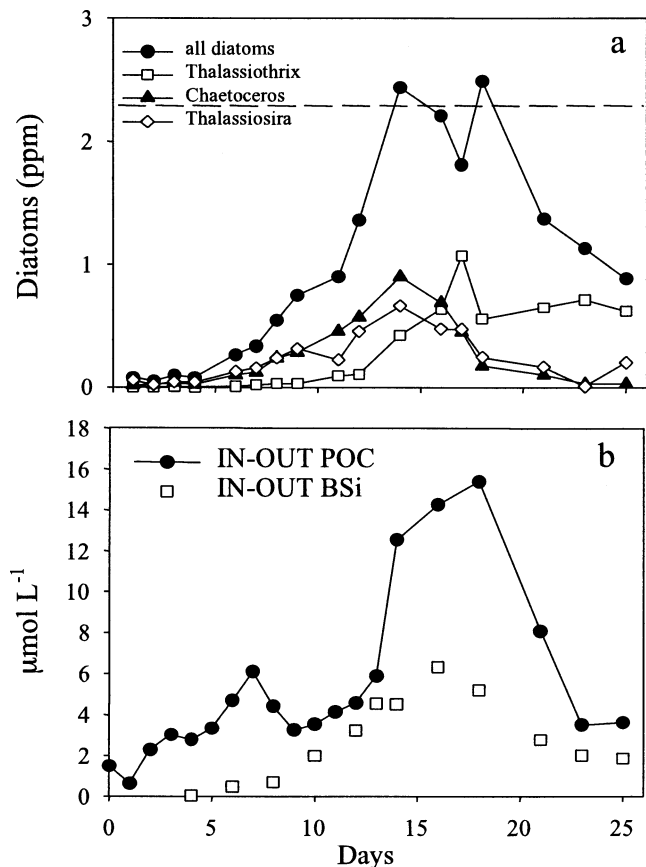
Fig. 3. (a) Diatom abundances at 5 m in depth in the patch for all diatoms, *Thalassiothrix longissima, Chaetoceros* spp., and *Thalassiosira* spp. The dashed line represents the predicted critical threshold (using a α of 1) for diatom abundances required to trigger the onset of algal aggregation (*see Methods*); (b) IN–OUT POC mean mixed-layer concentrations and IN–OUT BSi mean mixed-layer concentrations. There were no replicates for diatom enumeration; POC was derived from transmissivity (no replicates); but a CTD at the patch center on day 21 of SERIES indicated no significant variations among six profiles (Boyd et al. 2004). The standard error of the mean for BSi concentrations ($n = 3$) is smaller than the symbol size. Patch dilution (which reduced diatom, POC, and BSi concentrations) was not corrected for. The OUT data used for calculations were based on the mean of four time points obtained between days 1 and 15 for POC and three time points obtained between days 3 and 22 for BSi. There were only minor variations in both POC and BSi concentrations in the surface layer of the surrounding HNLC waters (Boyd et al. 2004).

cases, data sets on particle properties were only available for days 0–12 of SERIES (*see Materials and methods*). A dramatic shift in particle size spectra between days 0 and 12 was reflected in a marked increase in mean particle size (Fig. 6a), which was consistent with a floristic shift from small phytoplankton (Table 1) to large diatoms (Fig. 3a). Elevation of mean particle size was accompanied by a fivefold increase in particle abundance, comparable to observed increases in diatom stocks (Fig. 3a). Although based on a small data set, the sinking rates of the algal community in iron-enriched waters were less than those observed outside of the patch between days 1 and 12 (Fig. 6b). The sinking rates of the

dominant diatom species during the bloom were greater than community sinking rates (2.2 ± 0.4 to 3.1 ± 0.6 m d^{-1}; c.f. Fig. 6b), but were significantly slower inside the patch than in the surrounding waters (OUT sinking rates were 4.2 ± 0.4 m d^{-1}). The concentrations of TEP, exudates produced by phytoplankton, inside the patch were greater at all times than those in the surrounding waters (100–250 XG equiv. L^{-1} vs. 40–100 XG equiv. L^{-1}; Fig. 6c). The time series of TEP concentrations in the patch was relatively noisy, with no clear temporal trend(s) emerging. As the bloom developed, the Si : C ratios for particles in the mixed layer tripled until day 12, and thereafter they leveled off to around 0.35 (mol : mol) for the remainder of SERIES (Fig. 6d). In contrast, particles intercepted at 50 m in depth by surface-tethered free-drifting traps (*see* Boyd et al. [2004] for details) were around 0.4 (mol : mol) until day 14/15, at which time they doubled (by day 21) and declined to <0.4 by the end of SERIES (Fig. 6d).

Model simulations predicted that the critical particle concentration for algal aggregation (sensu Jackson and Lochmann 1992) was 2.3 ppm for a α of 1 and 23 ppm for a α of 0.1. The maximum diatom abundance observed during SERIES was 2.5 ppm during the period bounded by days 13 and 17 (Fig. 3a). Thus, using a α value of 1, the critical particle concentration for aggregation would have been exceeded between days 13 and 17 (*see* dashed horizontal line in Fig. 3a). In contrast, when a α value of 1 was assumed, aggregation would not have been initiated during the SERIES bloom. Based on the interplay of observed environmental conditions and algal properties such as growth rate, the model (using a α value of 1) predicted the onset of aggregation to be around day 12–13, along with a subsequent doubling in sinking rates resulting from the aggregation of diatoms (Fig. 7). If a α value of 0.1 was used, sinking rates would not increase during SERIES, as aggregation was never initiated (*see* caption, Fig. 7). The model simulations, therefore, indicate that the onset of mass diatom sedimentation would occur after day 15 ($\alpha = 1$) or not at all ($\alpha = 0.1$). Predicted sinking rates at the start of the bloom (i.e., OUT station) were similar to observed rates (Fig. 7, c.f. Fig. 6b). Although no sinking rate data were available after day 12, a marked increase in sinking rates is indicated by the observed rapid decrease in mixed-layer (25–30 m–thick) diatom abundances after day 17 (Fig. 3a). Ascribing a α value of 1 in the model provided the best prediction of both the critical particle threshold for aggregation and the timing of observed mass diatom sedimentation.

Bloom termination and decline—Time series of mixed-layer chlorophyll, POC, and BSi concentrations and diatom abundances indicate that the bloom peaked around days 16–17, then terminated, with a rapid decline in algal stocks thereafter (Figs. 2b, 3). The rapid decline of the bloom was observed from space, with a comparison of SeaWiFS daily images (modified to show algal carbon concentrations [μg L^{-1}] using measured C : chlorophyll ratios) on days 19 and 24 revealing a marked decrease in algal carbon concentrations over a 1,000 km^2 region (Fig. 8). Over this period, decreases in the mixed-layer POC inventory, corresponding to 80% of the iron-elevated POC during the bloom, were
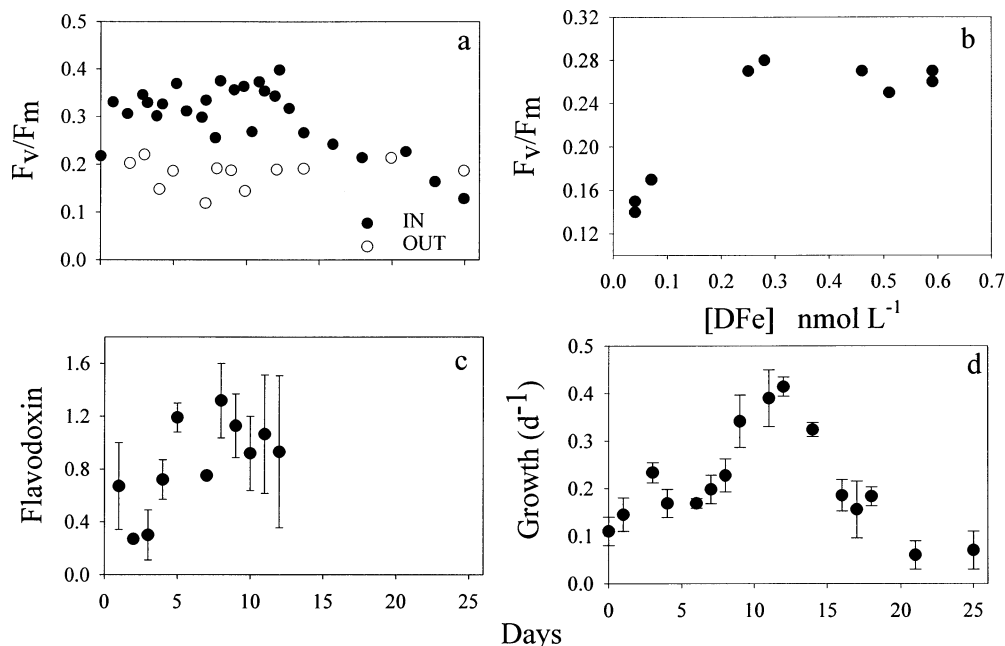
Fig. 4. (a) F_v/F_m mean mixed-layer concentrations; (b) F_v/F_m versus dissolved iron concentrations on day 7 during a nighttime underway ship survey; (c) IN patch diatom flavodoxin levels (at 5-m depth only—initially normalized to OUT flavodoxin levels, then normalized to diatom abundances)—i.e., a value of <1 corresponds to the alleviation of diatom iron stress; a value of 1 means that iron stress inside the patch is the same as OUT waters; (d) Algal net growth rates from algal C and ^{14}C estimates of NPP. The error bars represent the standard error of the mean ($n = 3$). In panels a and b, the error bars are smaller than the symbols.

observed (Figs. 3b, 8). During the bloom decline there was evidence of elevated POC concentrations below the mixed layer—consistent with sinking particles—prior to the observe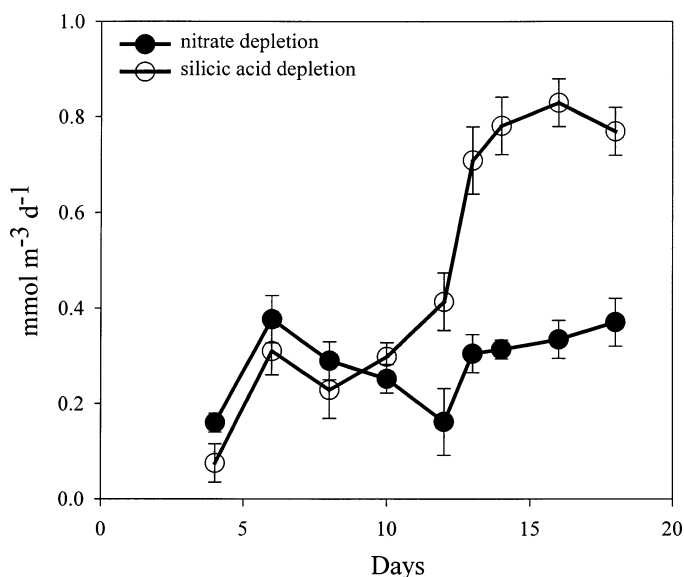d increase in downward POC flux in sediment traps at 50 m in depth (Fig. 9). The time scale of each phase of the bloom was 16–17 d for evolution and 1 to 2 d for termination, and there was a rapid decline phase of at least 5–6 d. We had to depart the SERIES site before the decline phase of the bloom was completed, with chlorophyll on day 25 being around 0.7 mg m^{-3} higher than initially observed (Fig. 2b) and the diatom community dominated by *Thalassiothrix longissima* (Fig. 3a).

Discussion

The phytoplankton bloom observed during SERIES provides insights into how iron enrichment influences bloom dynamics. In the following four sections, the main features of, and the factors controlling, the evolution, termination, and decline phases of the bloom will be elucidated, and their implications for modeling bloom dynamics will be presented. Our findings will be compared and contrasted with both iron-induced mesoscale blooms (e.g., Coale et al. 1996b) and other diatom blooms from both field (Lochte et al. 1993) and lab mesocosm (Alldredge et al. 1995) studies.

Key aspects of bloom evolution—Unlike the study of many naturally occurring blooms, the purposeful addition of iron to HNLC waters provides the factor triggering the bloom and offers the opportunity to study the onset of the bloom. During SERIES, a massive diatom bloom was observed, but initially the effect of iron enrichment was to promote transient increases in the abundances of small phy-

Fig. 5. Algal nitrate and silicic acid depletion estimated from changes in mixed-layer nutrient concentrations (*see Methods*) and subsequently corrected for patch dilution effects (Boyd et al. 2004). The error bars represent the standard error of the mean ($n = 3$).
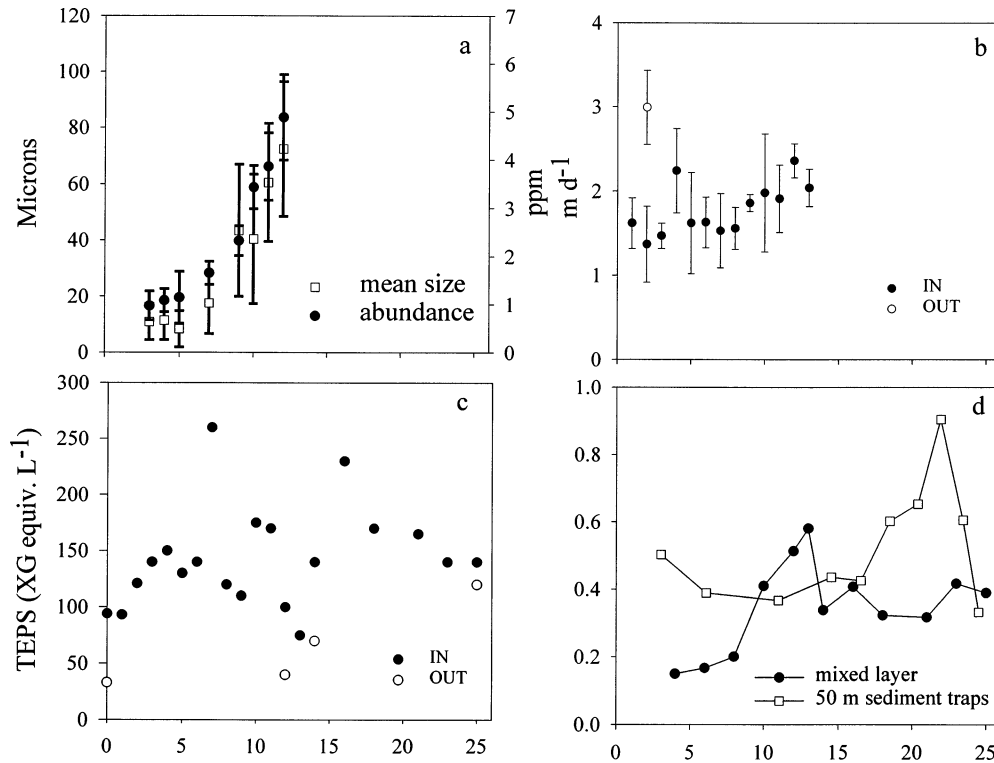
Fig. 6. (a) Mean particle size and abundance from samples at 5 m in depth; (b) algal sinking rates from samples at 5 m in depth; (c) TEP abundances (5-m depth) ; (d) PSi : POC ratios (mol : mol) for mixed-layer particles and sinking particles intercepted at 50 m in depth by a surface-tethered, free-drifting sediment trap. The error bars represent the standard error of the mean ($n = 3$). In panels c and d, the error bars are smaller than the symbols.
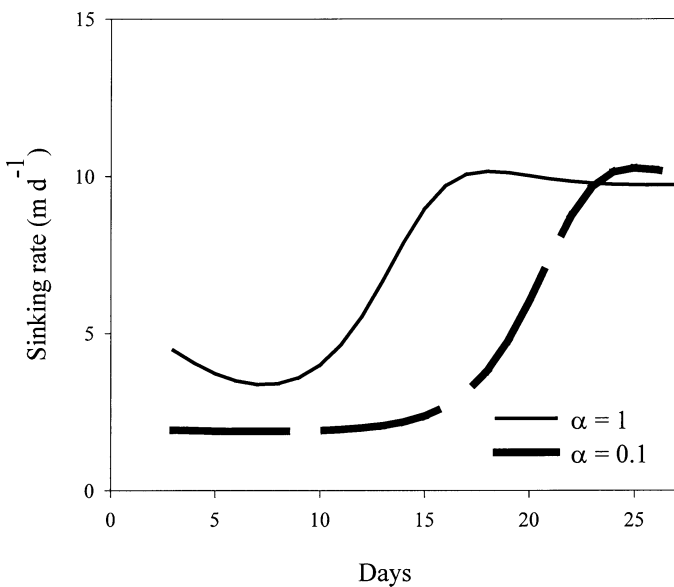

Fig. 7. Predicted time series of algal sinking rates from algal aggregation modeling (Jackson and Lochmann 1992) using a α of 1 and 0.1, in conjunction with data from SERIES (*see Methods*). Note in the simulation using a α of 0.1, the predicted increase in sinking rates after day 19 would not have occurred, as it is conditional on the critical particle concentration for algal aggregation (23 ppm for $\alpha = 1$) being exceeded (c.f. Fig. 3a).

toplankton—*Synechococcus* between days 1 and 3 and *E. huxleyi* from days 4 to 11. In contrast, the concurrent exponential increase in diatom stocks—comprising several species—took place for 16 d prior to bloom termination, around days 17–18. These community-wide increases in phytoplankton stocks are indicative of widespread iron limitation among the resident phytoplankton taxa at this HNLC site, as has been previously reported in mesoscale iron enrichments in tropical (Coale et al. 1996*b*) and polar (Boyd and Abraham 2001) HNLC waters. The changes in algal community structure observed during SERIES also provide further support, in a different oceanic province—subpolar waters—for the ecumenical Iron Hypothesis. During SERIES, the transient increases in small phytoplankton abundances reflect alleviation of iron algal limitation (i.e., bottom-up control), followed within a few days by top-down control via microzooplankton herbivory (Boyd et al. 2004). In contrast, iron supply and low grazing pressure permitted the diatoms stocks to increase exponentially to >5 μg chlorophyll L^{-1} (Boyd et al. 2004). Transient iron-mediated increases in the abundances of small phytoplankton, that were subsequently grazed down to ambient levels, have also been observed in other mesoscale iron enrichments in the equatorial Pacific (Landry et al. 2000) and the Southern Ocean (Boyd 2002).

A significant difference in SERIES (from previous iron enrichments) was the transient increase in coccolithophore

Fig. 9. A summary of POC stocks and downward export flux during the bloom termination and decline (days 16–25). (a) Mixed-layer POC stocks (note initial POC stocks were 0.6 g C m^{-2}); (b) daily change in POC stocks directly below the 25-m mixed layer observed over this period; (c) daily change in POC stocks between 35 m in depth and a free-drifting sediment trap (50-m depth); (d) change in the downward POC flux at 50 m in depth.
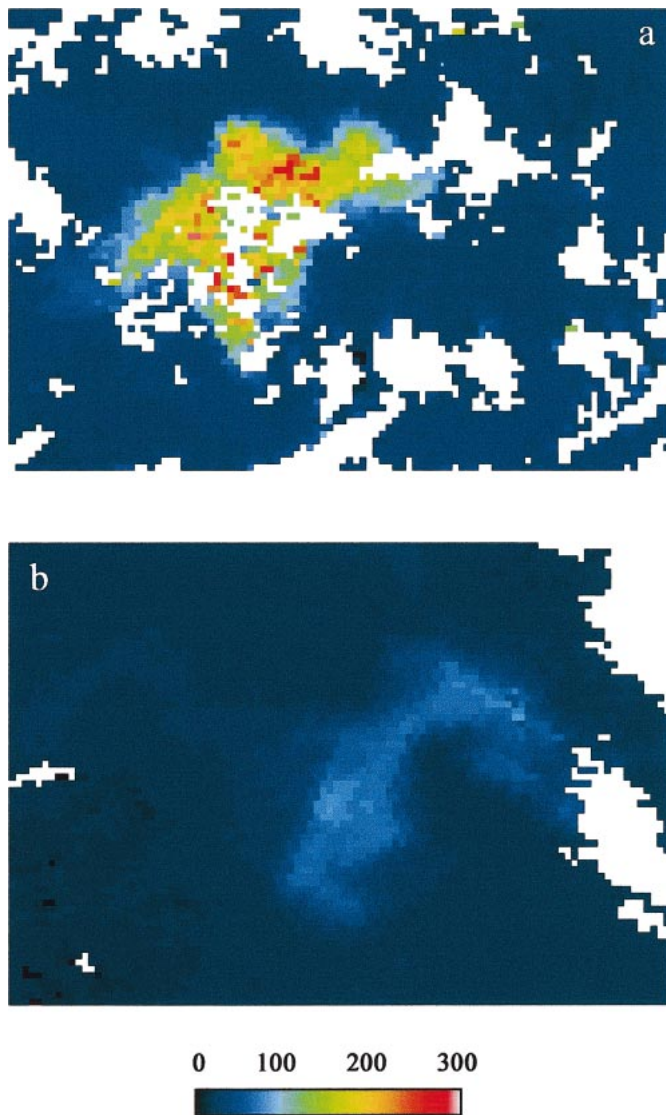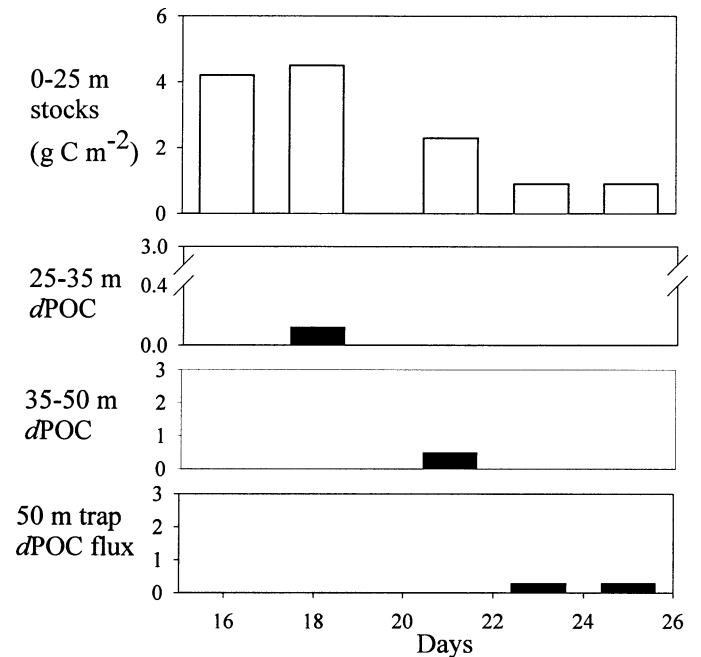

Fig. 8. Satellite images of the SERIES bloom on (a) day 19 and (b) day 24, derived initially from SeaWiFS ocean color then transformed to units of algal carbon using measured C : chlorophyll ratios corresponding to each day for the surface mixed layer. The units for the scale bar are μg algal C L^{-1}. The areal extent of the bloom was around 1,000 km^2 on day 19.

abundances, the growth rates of which are reported to be limited by cobalt rather than iron in northeast Atlantic waters (Ellwood and van den Berg 2001). Iron-mediated temporary increases in haptophyte stocks have been reported in both polar (Boyd 2002) and tropical (Landry et al. 2000) mesoscale iron enrichments, but at these sites the haptophytes were predominantly autotrophic nanoflagellates rather than coccolithophores (Landry et al. 2000; Boyd 2002). The temporal trends in algal community structure following iron enrichment of subpolar HNLC waters; of initial and transient increases in cyanobacterial abundances, followed by temporary increases in haptophyte abundances; and concurrent (but persistent) increases in diatom stocks are similar to those reported for both tropical and polar HNLC waters

(Boyd 2002). This is evidence of a common response to iron enrichment across these three types of HNLC oceanic provinces.

The diatoms, unlike the pico- and nano-phytoplankton, were not subjected to heavy grazing pressure (Boyd et al. 2004) and thus increased exponentially for 16 d. Early in the diatom bloom, there were marked physiological changes—in response to iron enrichment—evident from both F_v/F_m and diatom flavodoxin levels. The latter assay is particularly sensitive to diatom iron stress (Boyd and Abraham 2001), with transient decreases in flavodoxin levels observed after both iron infusions, followed by a rapid transition to higher flavodoxin levels at iron concentrations of 0.3–0.4 nmol L^{-1} (i.e., at these iron concentrations, F_v/F_m remained elevated). Moreover, flavodoxin levels were observed to increase after day 6, even though algal growth rates were increasing at this time (Fig. 4d). A similar temporal trend in flavodoxin levels and F_v/F_m was observed during SOIREE (Boyd and Abraham 2001).

During SERIES, we assumed that F_v/F_m is the most representative measure of algal iron limitation. The time series of F_v/F_m indicated that following iron enrichment, the alleviation of algal iron limitation lasted for 12 d, until dissolved iron declined to background concentrations for this HNLC region (Nishioka et al. 2001). The threshold (<0.2 Fe nmol L^{-1}) for the onset of algal iron limitation in SERIES is similar to that reported from nutrient uptake kinetic experiments in the HNLC equatorial Pacific (Coale et al. 1996a) and in FRRF studies during the SOIREE polar iron enrichment

(Boyd and Abraham 2001). The maximum values of F_v/F_m during SERIES (around 0.55 during an underway survey on day 4) were below the theoretical maximum (0.65 for diatoms; Behrenfeld et al. 1996) and were also less than the highest reported values during IronEx II (0.65; Behrenfeld et al. 1996) and SOIREE (0.64; Boyd and Abraham 2001). The beginning of iron limitation on day 12 was reflected by an increase in C : chlorophyll ratios and a decrease in algal net growth rates, as reported for IronEx II and SOIREE (*see* Boyd 2002). The concurrence of these changes with those in F_v/F_m supports our assumption that F_v/F_m is the most representative index of the impact of iron concentrations on algal physiology. Note, however, that although the early symptoms of algal iron limitation were apparent by day 13, iron limitation increased over the following 4 d, resulting in a progressive decrease in algal growth rates and F_v/F_m (Fig. 4).

The persistent decline in F_v/F_m during SERIES was also reported during the IronEx II experiment by Behrenfeld et al. (1996) when values decreased after day 4, even though the peak in chlorophyll concentrations was not observed until day 6 (Coale et al. 1996*b*). Similarly, during SERIES, algal stocks continued to increase for another 5–6 d after algal iron limitation commenced on day 12. This continued elevation of algal stocks was most likely due to several further divisions at rates ranging from 0.15 to 0.3 d^{-1} (Fig. 4d) by diatoms using intracellularly stored iron (Sunda and Huntsman 1995; Maldonado et al. 2002): total dissolvable iron—a proxy for particulate iron—was 0.4 nmol L^{-1} from day 12 until day 15 and decreased thereafter (Johnson unpubl. data). The use of intracellularly stored iron to maintain algal growth rates has previously been reported in lab culture studies of algal iron stress using *Synechococcus* sp. (Sandström et al. 2003). Sandström et al. (2003) report that upon transfer from iron-replete to iron-depleted conditions, increases in *Synechococcus* stocks were observed, as the iron-deficient cells continued to grow, albeit at a lower rate (relative to iron-replete cells) for several days. Moreover, similar trends have been observed in lab cultures of diatoms isolated from Southern Ocean HNLC waters (Strzepek unpubl. data).

A gradual transition, over 5–6 d, from iron-replete status to iron limitation in the phytoplankton community is evident from the progressive decrease in F_v/F_m after day 12. During this period, there were reductions in algal growth rate as well as rapid and pronounced increases in the algal uptake ratio of Si : NO$_3$ from unity to three. The latter trend has previously been widely reported from shipboard experiments in HNLC waters (e.g., Hutchins and Bruland 1998; Franck et al. 2000). However, in SERIES during this transition from iron-replete to iron-depleted conditions, silicic acid uptake rates increased significantly, with little change in nitrate uptake. This represents a marked departure from previously reported trends in the Si : NO$_3$ uptake stoichiometry during shipboard experiments in which "*The increase in the Si : NO$_3$ uptake ratio was mainly due to reduced nitrate use at low iron concentrations rather than enhancement of silicic acid uptake*" (Franck et al. 2000).

Thus, although the trends in Si : NO$_3$ algal uptake ratios are similar between SERIES and the shipboard experiments of Hutchins and Bruland (1998) and Franck et al. (2000),

the trends in algal nutrient uptake rates are not, with elevated silicic acid uptake being the main determinant of the increased uptake ratios during SERIES, rather than reduced nitrate uptake.

An important distinction between these shipboard Si : NO$_3$ uptake experiments (e.g., Hutchins and Bruland 1998; Franck et al. 2000) and SERIES is that in the latter, there was a transition from iron-replete to iron-limited conditions, whereas in the former, the bottle treatments were either iron-replete or iron depleted. This may account for the departure in the reported trends in silicic acid and nitrate uptake, which in SERIES may have been driven by changes in diatom physiology and/or floristics during the 5-d transition to iron limitation. For example, there was a marked increase in *Thalassiothrix longissima* abundances between days 12 and 16, concurrent with lesser changes in the abundance of other dominant diatom species. Thus, it is difficult to interpret the observation that silicic acid uptake rates, even when normalized to BSi, display a slight but significant increase from days 10–12 (0.08 ± 0.01 mmol Si [mmol BSi]$^{-1}$ d^{-1}) to days 13–15 (0.13 to 0.15 ± 0.03 mmol Si [mmol BSi]$^{-1}$ d^{-1}) over this transition period. This increase in silicic uptake after day 12 of SERIES resulted in marked depletion of the mixed-layer silicic acid inventory and thus was probably pivotal in determining the onset of bloom termination. These findings point to the need to better resolve the relative influence of diatom physiology and floristics on nutrient uptake stoichiometry. More data are required on the uptake rates and kinetics of key HNLC diatoms under a range of algal iron stress—akin to that carried out on non-HNLC diatoms by Brzezinski (1985).

The evolution phase of the subarctic SERIES bloom was of around 16 d in duration, which is intermediate between that observed in mesoscale iron enrichments in tropical (6–7 d) and polar HNLC waters (>25 d) (Boyd 2004). The role of temperature in setting maximum algal growth rates (Banse 1991) accounts for many of these differences in bloom dynamics (Boyd 2002). The SEEDS bloom in the northwest subarctic Pacific evolved over 12 d (Boyd 2004) and attained exceptionally high chlorophyll levels of >20 μg L^{-1}, in a 10-m mixed layer, relative to the results of the present study. The results of the SEEDS experiment are indicative of the key role that other environmental factors, such as mixed-layer depth, play in setting not only the magnitude of iron-mediated blooms but also their time scale of development (Boyd 2002).

Drivers of bloom termination—nutrients and/or grazers?—Phytoplankton blooms may be terminated by bottom-up and/or top-down control (Cullen 1991). In the case of SERIES, the exponential increase in diatom stocks, low rates of herbivory on diatoms (Boyd et al. 2004), the detection of iron limitation on day 12, and the subsequent depletion of much of the mixed-layer silicic acid inventory point to bloom termination due to bottom-up control. Initially, reduced iron concentrations resulted in the onset of algal iron limitation that led to a slowing of algal growth rates. However, as silicic acid was rapidly depleted by day 15/16, bloom termination may have been triggered by simultaneous limitation of diatom growth by both iron and silicic acid

supply. Only one other mesoscale study—IronEx II—has recorded both the evolution and termination phases of an iron-mediated bloom (note that the SOFEX–North bloom in the subpolar Southern Ocean was not considered here, as it was probably terminated by a physical mechanism—subduction of the bloom; Boyd 2004). During IronEx II, the bloom terminated after 7–8 d (Coale et al. 1996b). There are some similarities between the trends observed in both IronEx II and SERIES prior to and during the bloom termination. A marked decrease in F_v/F_m was reported during IronEx II (Behrenfeld et al. 1996) and was initially due to decreased dissolved iron concentrations (Behrenfeld et al. 1996; Coale et al. 1996b). However, silicic acid was also depleted to <1 μmol L^{-1} during IronEx II (Wells 2002), indicating a similar transition from iron limitation of algal growth to simultaneous limitation by silicic acid and iron supply as a trigger for bloom termination. Landry et al. (2000) report that the impact of microzooplankton herbivory (in particular by heterotrophic dinoflagellates) on the dominant diatom in the IronEx II bloom—*Pseudo-Nitzshia*—was responsible for the demise of the bloom. It is therefore likely that both bottom-up and top-down factors terminated the IronEx II bloom.

Shipboard studies of naturally occurring blooms have observed similar trends to those reported for IronEx II or SERIES. The former is akin to a bloom near the Polar Front (Pacific sector of the Southern Ocean), monitored with an array of 10 bio-optical moorings during the AESOPS program, whose decline was attributed to both bottom-up and top-down control (Abbott et al. 2000). In contrast, the termination of the SERIES bloom by bottom-up control is similar to that reported for the 1989 spring diatom bloom in the northeast Atlantic, which was terminated by silicic acid depletion (Lochte et al. 1993). The ability to remove silicic acid to vanishingly low levels is probably due to diatoms having specific properties, such as the ability to alter the thickness of their frustules (Martin-Jezequel et al. 2000), and/or species that exhibit widely differing silica uptake kinetics (Brzezinski 1985). During SERIES, there was species succession in diatoms around day 15, when silicic acid was at low concentrations.

The SERIES data sets indicate that the timing of bloom termination could have been altered had more iron been added to the patch. Specifically, the increase in silicic acid uptake rates—which resulted in the depletion of silicic acid to low concentrations—occurred during the transition from iron-replete to iron-limited conditions. Thus, had a third iron infusion taken place on day 12 of SERIES, the algal $Si:NO_3$ uptake ratio may have remained close to unity, potentially extending the bloom evolution phase, as silicic acid uptake rates would have remained several-fold lower. However, it is not known how a further iron addition might have affected diatom physiology or species succession.

Bloom termination and decline—the role of particle dynamics—Particle dynamics, although not usually classified as bottom-up control, are also thought to be a key determinant of the timing of the latter phases of algal blooms. The potential mechanisms controlling the termination and decline of blooms have been studied in considerable detail using lab mesocosms (Alldredge et al. 1995; Prieto et al. 2002). Some

of the commonly reported trends in such mesocosm experiments include (a) bloom termination being driven by mass sedimentation (Alldredge et al. 1995) or nutrient limitation (bloom 2 in Prieto et al. 2002), or jointly by both processes (bloom 1 in Prieto et al. 2002); (b) the role of TEP in the formation of rapidly sinking aggregates (Kiorboe and Hansen 1993; Alldredge et al. 1995); (c) a time lag of 1–3 d between the peak in diatom abundances and a subsequent peak in the abundances of aggregates (Prieto et al. 2002); and (d) species succession during diatom blooms (Alldredge et al. 1995) and how succession influences the composition of aggregates via 'sequential aggregation' (Passow 1991; Crocker and Passow 1995). Some of these trends observed in mesocosms, such as species succession and the subsequent composition of aggregates (Riebesell 1991), have also been reported in coastal diatom blooms, mainly from studies in the Baltic Sea.

Our highly resolved observations within the SF_6 labeled patch provide a valuable comparison with the key findings of these lab mesocosm and coastal studies. During SERIES there was evidence of both nutrient limitation (iron commencing on day 12, silicic acid on days 15–16) and mass sedimentation (from a modeling simulation, sedimentation was initiated around days 15–16 and was evident as the observed rapid decline in stocks after day 18). However, it is not possible to clearly attribute the termination of the SERIES bloom to either a single or multiple factors because of the temporal overlap between these causal mechanisms. Moreover, as the critical particle threshold for aggregation (Jackson and Lochmann 1992) is set by a range of factors including mixed-layer depth, shear, algal geometry, growth rate, and α, it is likely that nutrient limitation and algal aggregation are inextricably linked. For example, the onset of iron (and or silicic acid) limitation of phytoplankton growth may have elevated the α of diatoms and thus accelerated the initiation of algal aggregation. Relationships between enhanced algal nutrient stress (mainly nitrate) and increased α have been observed in coastal diatoms (Kiorboe et al. 1990). However, Kiorboe et al. (1990) reported a wide range of species-specific relationships between nutrient limitation and α. Research is needed to first ascertain whether iron and/or silicic acid limitation alters the α of phytoplankton and, second, whether this relationship varies between species.

Mesocosm studies have shown exponential increases in TEP concentrations during the evolution, termination, and decline phases of blooms (Passow and Alldredge 1995; Prieto et al. 2002), which are thought to play an indirect role in initiating aggregation (Crocker and Passow 1995). However, during SERIES, there were no clear trends in TEP abundances over the phases of bloom development, termination, and decline, but abundances were higher than in the surrounding HNLC waters. One explanation for the lack of temporal trends in TEP concentrations between days 0 and 12 of SERIES is that the exponential increase in diatom abundances was concurrent with transient increases in other taxa, such as the haptophytes (including *Phaeocystis* spp., which are reported to produce high amounts of TEP; Hong et al. 1997). Significantly, TEP concentrations throughout all bloom phases of SERIES were an order of magnitude lower than reported from coastal diatom blooms of similar mag-

nitude (i.e., chlorophyll >6 μg L^{-1}; Engel 2000). This indicates that trends observed in coastal blooms or in lab mesocosm experiments may not be readily applicable to open ocean or HNLC waters, in which iron and/or silicic acid may control algal nutrient limitation. Although TEP production has been linked to nitrate limitation for some coastal diatom species in lab cultures, there are reports of wide variations in algal α between species (Kiorboe and Hansen 1993), and as far as we know, no published study has investigated the relationship between diatom iron stress and TEP production or algal α. Despite the lack of change in TEP abundance during SERIES, there was evidence of algal aggregation and mass sedimentation during the bloom.

The rapid decline of the SERIES bloom within a 25–30-m mixed layer over 4–5 d is indicative of a pronounced increase in particle sinking speeds over those observed earlier in the bloom for phytoplankton (2 m d^{-1}) and as predicted by the aggregation model (10 m d^{-1}). Indeed, by days 20–21, a marked increase in both diatom abundances (for example, *Thalassiosira* spp. increased from 2,700 cells mL^{-1} to 19,400 cells mL^{-1} in trap cups between trap deployments 2.5 d apart) and diatom aggregates (from 500 to $>7,000$ mL^{-1}) were observed in the surface-tethered, free-drifting traps at 50 m in depth. This is indicative both of rapid sinking of cells and of a 3–4-d lag between corresponding peaks in diatom abundance in the upper ocean and in the number of settling aggregates and cells, as previously reported in lab diatom mesocosms (Prieto et al. 2002).

There was evidence of species succession during the SERIES diatom bloom, with decreases in both *Thalassiosira* and *Chaetoceros* spp. after days 14–15 and concurrent increases in *T. longissima* abundances within the mixed layer. On days 20–21, the aggregates intercepted by the traps at 50 m in depth were dominated by *Thalassiosira* and *Chaetoceros* spp., with few *T. longissima* ($>7,000$ mL^{-1} vs. <100 mL^{-1} for *T. longissima*). On day 23, on the other hand, in the 50-m traps, *Thalassiothrix* aggregates had increased >50-fold, with relatively little change in the number of aggregates dominated by *Thalassiosira* and *Chaetoceros* spp. Again, the trends in SERIES appear to support observations from lab mesocosm experiments (Alldredge et al. 1995) and in coastal ocean diatom blooms (Riebesell 1991) with regard to the impact of algal species succession on the resulting composition of algal aggregates.

The observed species succession during SERIES may be symptomatic of links to both nutrient limitation and aggregation (Prieto et al. 2002) and of the assertion that the aggregation of diatoms may not "*necessarily involve the entire diatom community simultaneously, but which can successively affect individual species*" (Riebesell 1991).

Although little is known about the iron or silicic acid uptake kinetics of many HNLC open-ocean diatom species, in the case of *T. longissima* (a cylinder of 3.8 μm in diameter and with a height of 2,000 μm), cellular geometry may favor the sequestration of these elements at low concentrations. Furthermore, the mixed-layer abundances of *T. longissima* remained relatively constant between days 17 and 25, a period characterized by both low iron and silicic acid concentrations and elevated downward fluxes of diatom aggregates, POC, and BSi at 50 m in depth (Boyd et al. 2004), sup-

porting Riebesell's observation. Clearly, more lab culture studies on a wide range of these HNLC open-ocean diatoms are needed to further elucidate some of the links between species succession, iron, and/or silicic acid limitation and algal aggregation.

The decline phase of the SERIES bloom was most likely initiated by algal aggregation followed by sedimentation. Insights into the fate of this material are provided by rapid changes in the biogeochemical properties of settling particles (Fig. 6d). After day 15, trends in the Si:C ratios of settling particles at 50-m depth were not reflected by those for mixed-layer particles, nor were they explained by a 1–2-d lag due to particles sinking. Furthermore, as the Si:C ratios of intercepted sinking particles were invariant between 50 and 125 m in depth over this period (Boyd et al. 2004), major changes in particle composition probably occurred only between 25 and 50 m in depth. Particulate ratios are influenced by preferential removal of POC relative to opal by biota such as heterotrophic bacteria (Bidle and Azam 2000; Bidle et al. 2002) or modification of particle carbon content via the incorporation of TEP during aggregation (Passow et al. 1994). In our study, particulate Si:C ratios were generally higher at 50 m relative to those at 0–25 m, consistent with preferential POC removal by heterotrophic bacteria, which probably controlled the fate of the majority of the exported POC (Fig. 9; present study; Boyd et al. 2004). However, bacterial POC removal is inconsistent with decreasing Si:C ratios at 50 m in depth after day 21. Possible explanations include a decrease in bacterial and/or grazing activity between 25 and 50 m, a change in the diatom species that were exported, and/or offsetting selective organic carbon removal from particles with carbon from TEP. Although the temporal trends for TEP were generally inconclusive, the SERIES mixed-layer inventory of TEP carbon declined by 35% between days 16 and 23, and thus TEP may have elevated the carbon content of settling particles during the bloom decline.

The highly resolved temporal and vertical data sets from SERIES provide insights into the functioning of the oceanic silica pump in HNLC waters. We recorded rapid changes in both Si:NO$_3$ uptake stoichiometry and mixed-layer particulate Si:C ratios during different bloom phases. Furthermore, Si:C particulate ratios were altered dramatically at shallower depths (i.e., <50 m) than were studied in previous investigations (Nelson et al. 2002). More information is required on how particulate Si:C ratios are altered, and lab culture studies are needed to characterize diatom species-specific Si:NO$_3$ and Si:C cellular ratios over a wide range of algal iron stress.

There have now been nine published mesoscale iron enrichments in HNLC waters. However, in only two cases has the bloom decline been observed—in detail during the present study (Boyd et al. 2004) and in IronEx II (Coale et al. 1996*b*; Bidigare et al. 1999). Both of these studies indicate that the lag phase between the bloom termination and the onset of export is on the order of days for tropical or subpolar waters. In the case of mesoscale experiments in polar HNLC waters, their longevity exceeded those of SERIES and IronEx II, but neither the bloom termination nor decline phases were observed (*see* summary in Boyd [2004]). Thus,

the lag time between the bloom termination and the onset of elevated export is not known for polar HNLC waters.

The absence of bloom termination and decline phases in polar iron enrichments is probably due to a combination of factors, including reduced algal growth rates at low temperatures (Boyd 2002), and in particular to the impact of entrainment of the surrounding HNLC waters into the iron-enriched patch as it expands via strain and rotation (Boyd 2002). Entrainment is an artefact of this experimental approach, as the areal extent of the patch (initially around 70 km²) may increase by more than a 10-fold measure (Boyd et al. 2004), resulting in a dilution of phytoplankton stocks to levels that are insufficient to attain the critical threshold for algal aggregation (Boyd et al. 2002), and/or to supply potentially limiting macronutrients such as silicic acid to the patch (Boyd 2002). This artefactual condition, although diluting the initially added iron (Boyd 2002), favors the persistence of a bloom in which chlorophyll concentrations remain elevated and constant (Boyd 2004) and has thus been likened to an algal chemostat culture (Boyd 2002; Boyd et al. 2002). Under such artefactual conditions, the definitions of bloom phases of evolution (i.e., increasing stocks) and termination (i.e., inflection point between evolution and decline) are no longer meaningful.

Implications for modeling blooms in the present and geological past—A key issue to be addressed is how the findings of recent mesoscale iron experiments relate to different environmental conditions in the geological past (Martin 1990) or to future climate-mediated changes in iron supply. The supply of iron in the geological past, inferred from dust records in cores such as Vostok, was considerably higher during the glacial maxima (Martin 1990). Is it possible to upscale the results from contemporary iron enrichments and relate them to the geological record? There have been suggestions that sustained periods (decadal to centennial) of iron-elevated productivity would result in a long-term adaptive response by zooplankton grazers, as observed in upwelling regions (Frost 1996), and, hence, in the gradual evolution of a ''high-productivity low-biomass'' system under top-down control. However, this view is at odds with the exceptional longevity of recurring diatom blooms in the geological record—inferred from 1-m–thick diatom oozes and accompanying barium enrichment (i.e., evidence of elevated export of POC)—such as in the northeast subarctic Pacific (Macdonald et al. 1999). The SERIES observations of the role of iron limitation in increasing the uptake of silicic acid, and the onset of bloom termination by both iron and silicic acid limitation, point to the need for more information from the geological record with regard to the nature of iron supply (episodic vs. persistent) and more information on mechanisms to concurrently supply both of these nutrients (Martin 1990; c.f. Harrison 2001). However, resolving the nature of nutrient supply from the geological record is problematic because of the need for very high temporal data resolution (c.f. Martin 1990).

In order to predict how future changes in iron supply to the ocean will affect bloom dynamics and the subsequent biogeochemical signature, we must first be able to adequately simulate the phases of iron-mediated blooms. Modeling

studies have so far used the results from mesoscale iron enrichments, such as SOIREE, to validate their simulations of the functioning of the polar HNLC ocean and to investigate how different iron-enrichment strategies might influence the outcome of these mesoscale studies (Hannon et al. 2001). This approach has resulted in promising simulations of biogeochemical observations during bloom evolution, but in contrast, simulations of bloom termination and decline phases were less successful. In particular, parameterization of the factors responsible for the bloom termination—such as iron supply—and the potential causal links with algal aggregation and sinking rates were problematic (Hannon et al. 2001). In part, this is the result of the lack of current understanding of these complex relationships and of the fact that parameterization of a process such as algal aggregation often requires a specialized model (Jackson and Lochmann 1992) that is computationally expensive to embed into another model. As previously stated, more lab and field data are needed on algal nutrient stress and their impact on algal α and subsequent aggregation in order to improve models of the fate of iron-mediated blooms in HNLC regions.

References

ABBOTT M. R., J. G. RICHMAN, R. M. LETELIER, AND J. S. BARTLETT. 2000. The spring bloom in the Antarctic polar frontal zone as observed from a mesoscale array of bio-optical sensors. Deep-Sea Res. II **47:** 3285–3314.

AGRAWAL, Y. C., AND H. C. POTTSMITH. 2000. Instruments for particle size and settling velocity observations in sediment transport. Mar. Geol. **168:** 89–114.

ALLDREDGE, A. L., C. GOTSCHALK, U. PASSOW, AND U. RIEBESELL. 1995. Mass aggregation of diatom blooms: Insights from a mesocosm study. Deep-Sea Res. II **42:** 9–27.

BANSE, K. 1991. Rates of phytoplankton cell division in the field: Iron enrichment experiments. Limnol. Oceanogr. **36:** 1886–1898.

BEHRENFELD, M. J., A. J. BALE, Z. S. KOLBER, J. AIKEN, AND P. G. FALKOWSKI. 1996. Confirmation of iron limitation of phytoplankton photosynthesis in the equatorial Pacific Ocean. Nature **383:** 508–510.

BIDIGARE, R. R., AND OTHERS. 1999. Iron-stimulated changes in ¹³C fractionation and export by equatorial Pacific phytoplankton. Paleoceanography **14:** 589–595.

BIDLE, K. D., M. MANGANELLI, AND F. AZAM. 2002. Regulation of oceanic silicon and carbon preservation by temperature control on bacteria. Science **298:** 1980–1984.

BIENFANG, P. K. 1981. Setcol; A technologically simple and reliable method for measuring phytoplankton sinking rates. Can. J. Fish. Aquat. Sci. **38:** 1289–1294.

BISHOP, J. K. B. 1999. Transmissiometer measurement of POC. Deep-Sea Res. I **46:** 353–369.

BOYD, P. W. 2002. The role of iron in the biogeochemistry of the Southern Ocean and equatorial Pacific: A comparison of in situ iron enrichments. Deep-Sea Res. II **49:** 1803–1822.

———. 2004. Ironing out algal issues in the Southern Ocean. Science **304:** 396–397.

———, AND E. R. ABRAHAM. 2001. Iron-mediated changes in phytoplankton photosynthetic competence during Soiree. Deep-Sea Res. II **48:** 2529–2550.

———, G. A. JACKSON, AND A. WAITE. 2002. Are mesoscale perturbation experiments in polar waters prone to physical arte-

facts? Evidence from algal aggregation modelling studies. Geophys. Res. Lett. **29:** doi: 10.1029/2001gl014210.

————, AND OTHERS. 2004. The decline and fate of an iron-induced subarctic phytoplankton bloom. Nature **428:** 549–553.

BRZEZINSKI, M. A. 1985. The Si : C : N ratio of marine diatoms interspecific variability and the effect of some environmental variables. J. Phycol. **21:** 347–357.

BUESSELER, K. O., AND OTHERS. 2001. Upper ocean export of particulate organic carbon and biogenic silica in the Southern Ocean along 170°W. Deep-Sea Res. II **48:** 4247–4273.

COALE, K. H., S. E. FITZWATER, AND R. M. GORDON. 1996*a*. Control of community growth and export production by upwelled iron in the equatorial Pacific. Nature **379:** 621–624.

————, AND OTHERS. 1996*b*. A massive phytoplankton bloom induced by an ecosystem-scale iron fertilization experiment in the equatorial Pacific Ocean. Nature **383:** 495–501.

CROCKER, K. M., AND U. PASSOW. 1995. Differential aggregation of diatoms. Mar. Ecol. Prog. Ser. **117:** 249–257.

CULLEN, J. J. 1991. Hypothesis to explain high-nutrient conditions in the open sea. Limnol. Oceanogr. **36:** 1578–1599.

ELLWOOD, M. J., AND C. M. G. VAN DEN BERG. 2001. Determination of organic complexation of cobalt in seawater by C.S.V. Mar. Chem. **75:** 33–47.

ENGEL, A. 2000. The role of transparent exopolymer particles (TEP) in the increase in apparent particle stickiness (α) during the decline of a diatom bloom. J. Plankton Res. **22:** 485–497.

FRANCK, V. M., M. A. BRZEZINSKI, K. H. COALE, AND D. M. NELSON. 2000. Iron and silicic acid availability regulate Si uptake in the Pacific sector of the Southern Ocean. Deep-Sea Res. II **47:** 3315–3338.

FROST, B. W. 1996. Phytoplankton bloom on iron rations. Nature **383:** 475–476.

HANNON, E., P. W. BOYD, M. SILVOSO, AND C. LANCELOT. 2001. Modeling the bloom evolution and carbon flows during Soiree: Implications for future in situ iron-enrichments in the southern ocean. Deep-Sea Res. II **48:** 2745–2774.

HARRISON, K. G. 2000. Role of increased marine silica input on paleo-pCO$_2$ levels. Paleoceanography **15:** 292–298.

HONG, Y., W. O. SMITH, JR., AND A-M. WHITE. 1997. Studies on transparent exopolymer particles (TEP) produced in the Ross Sea (Antarctica) and by *Phaeocystis antarctica* (*Prymnesiophyceae*). J. Phycol. **33:** 368–376.

HUTCHINS, D. A., AND K. W. BRULAND. 1998. Iron-limited diatom growth and Si : N uptake ratios in a coastal upwelling regime. Nature **393:** 561–564.

JACKSON, G. A., AND S. E. LOCHMANN. 1992. Effect of coagulation on nutrient and light limitation of an algal bloom. Limnol. Oceanogr. **37:** 77–89.

JACKSON, G. A. 2005. Coagulation theory and models of oceanic plankton aggregation, p. 271–291. *In* I. Droppo, G. Leppard, S. Liss, and T. Milligan [eds.], Flocculation in natural and engineered environmental systems. CRC Press.

KIØRBOE, T., K. P. ANDERSEN, AND H. G. DAM. 1990. Coagulation efficiency and aggregate formation in marine phytoplankton. Mar. Biol. **107:** 235–245.

————, AND J. L. S. HANSEN. 1993. Phytoplankton aggregate formation: Observations of patterns and mechanisms of cell sticking and the significance of exopolymeric material. J. Plankton Res. **15:** 993–1018.

LANDRY, M. R., J. CONSTANTINOU, M. LATASA, S. L. BROWN, R. R. BIDIGARE, AND M. E. ONDRUSEK. 2000. Biological response to iron fertilization in the eastern equatorial Pacific (Ironex II). iii. Dynamics of phytoplankton growth and microzooplankton grazing. Mar. Ecol. Prog. Ser. **201:** 57–72.

LAROCHE, J., P. W. BOYD, R. M. L. MCKAY, AND R. J. GEIDER. 1996. Flavodoxin as an in situ marker for iron stress in phytoplankton. Nature **382:** 802–805.

LAW, C. S., A. J. WATSON, M. I. LIDDICOAT, AND T. STANTON. 1998. Sulphur hexafluoride as a tracer of biogeochemical and physical processes in an open-ocean iron fertilisation experiment. Deep-Sea Res. II **45:** 977–994.

LOCHTE, K., H. W. DUCKLOW, M. J. R. FASHAM, AND C. STIENEN. 1993. Plankton succession and carbon cycling at 47°N 20°W during the JGOFS North Atlantic Bloom Experiment. Deep-Sea Res. II **40:** 91–114.

MALDONADO, M. T., AND OTHERS. 2001. Iron uptake and physiological response of phytoplankton during a mesoscale Southern Ocean iron enrichment. Limnol. Oceanogr. **46:** 1802–1808.

MARTIN, J. H. 1990. Glacial-interglacial CO$_2$ change: The iron hypothesis. Paleoceanography **5:** 1–13.

MARTIN-JEZEQUEL, V., M. HILDEBRAND, AND M. A. BRZEZINSKI. 2000. Silicon metabolism in diatoms: Implications for growth. J. Phycol. **36:** 821–840.

MCDONALD, D., T. F. PEDERSEN, AND J. CRUSIUS. 1999. Multiple late quaternary episodes of exceptional diatom production in the Gulf of Alaska. Deep-Sea Res. II **46:** 2993–3017.

NELSON, D. M., AND OTHERS. 2002. Vertical budgets for organic carbon and biogenic silica in the pacific sector of the Southern Ocean, 1996–1998. Deep-Sea Res. II **49:** 1645–1674.

NISHIOKA, J., S. TAKEDA, C. S. WONG, AND W. K. JOHNSON. 2001. Size-fractionated iron concentrations in the Northeast Pacific Ocean: Distribution of soluble and small colloidal iron. Mar. Chem. **74:** 157–179.

PASSOW, U. 1991. Species-specific sedimentation and sinking velocities of diatoms. Mar. Biol. **108:** 449–455.

————, AND A. L. ALLDREDGE. 1995. A quantitative way to determine the concentration of transparent exopolymer particles (TEP). Limnol. Oceanogr. **40:** 1326–1335.

————, B. E. LOGAN, AND A. ALLDREDGE. 1994. The role of particulate carbohydrate exudates in the flocculation of diatom blooms. Deep-Sea Res. I **41:** 335–357.

PRIETO, L., AND OTHERS. 2002. Scales and processes in the aggregation of diatom blooms: High time resolution and wide size range records in a mesocosm study. Deep-Sea Res. I **49:** 1233–1253.

RIEBESELL, U. 1991. Particle aggregation during a diatom bloom. II. biological aspects. Mar. Ecol. Prog. Ser. **69:** 281–291.

SANDSTRÖM, S., A. G. IVANOV, Y. I. PARK, G. ÖQUIST, AND P. GUSTAFSSON. 2002. Iron stress responses in the cyanobacterium *Synechococcus* sp. pcc7942. Physiol. Plant. **116:** 255–263.

STERNER, R.W., T.M. SMUTKA, R. M. L. MCKAY, Q. XIAOMING, E. T. BROWN, AND R. M. SHERRELL. 2004. Phosphorus and trace metal limitation of algae and bacteria in Lake Superior. Limnol. Oceanogr. **49:** 495–507.

SUNDA, W. G., AND S. A. HUNTSMAN. 1995. Iron uptake and growth limitation in oceanic and coastal phytoplankton. Mar. Chem. **50:** 189–206.

WELLS, M. L. 2003. The level of iron enrichment required to initiate diatom blooms in HNLC waters. Mar. Chem. **82:** 101–114.